Journal of Power Sources 249 (2014) 440–445

Contents lists available at ScienceDirect

Journal of Power Sources

journal homepage: www.elsevier.com/locate/jpowsour

Different electrode configurations to optimize performance of multi-electrode microbial fuel cells for generating power or treating domestic wastewater

Yongtae Ahn, Marta C. Hatzell, Fang Zhang, Bruce E. Logan*

Department of Civil & Environmental Engineering, Penn State University, 212 Sackett Building, University Park, PA 16802, USA

HIGHLIGHTS

- Comparison of different electrode configurations with MFCs treating wastewater.
- Closer electrode configuration produced higher power and coulombic efficiency.
- Spaced electrode configuration reduced wastewater treatment time.
- Transport within SPA and SEA reactors modeled through computer simulations.
- Oxygen transport and hindered substrate diffusion increased treatment time.

ARTICLE INFO

Article history:
Received 18 September 2013
Received in revised form
16 October 2013
Accepted 17 October 2013
Available online 5 November 2013

Keywords:
Microbial fuel cell
Domestic wastewater
Electrode distance
Coulombic efficiency
Substrate diffusion
Model simulation

ABSTRACT

Scaling-up of microbial fuel cells (MFCs) for practical applications requires compact, multiple-electrode designs. Two possible configurations are a separator electrode assembly (SEA) or closely spaced electrodes (SPA) that lack a separator. It is shown here that the optimal configuration depends on whether the goal is power production or rate of wastewater treatment. SEA MFCs produced a 16% higher maximum power density (328 ± 11 mW m^{-2}) than SPA MFCs (282 ± 29 mW m^{-2}), and higher coulombic efficiencies (SEAs, 9–31%; SPAs, 2–23%) with domestic wastewater. However, treatment was accomplished in only 12 h with the SPA MFC, compared to 36 h with the SEA configuration. Ohmic resistance was not a main factor in performance as this component contributed only 4–7% of the total internal resistance. Transport simulations indicated that hindered oxygen diffusion into the SEA reactor was the primary reason for the increased treatment time. However, a reduction in the overall rate of substrate diffusion also may contribute to the long treatment time with the SEA reactor. These results suggest that SEA designs can more effectively capture energy from wastewater, but SPA configurations will be superior in terms of treatment efficiency due to a greatly reduced time needed for treatment.

1. Introduction

Microbial fuel cells (MFCs) are an emerging method for achieving sustainable wastewater treatment technology since they can remove organic matter and simultaneously generate electricity [1–3]. Single-chamber, air–cathode MFCs are the most promising design for practical applications because they use passive oxygen transfer to the cathode as an electron acceptor, and the single-chamber design avoids the need for a membrane. MFCs designs that are compact (narrow chamber width) and that have multiple anodes are essential to achieve efficient power generation and shorter hydraulic retention times [4–7].

The type and spacing of the electrodes are critical factors for achieving compact and scalable MFCs [8]. Decreasing the distance between the electrodes can improve power output by reducing solution (ohmic) losses [9–11]. Close electrode spacing could be especially important for domestic wastewater treatment as its conductivity is very low ($\sim$1 mS cm^{-1}), and therefore widely spaced electrodes would result in high ohmic losses. Very closely spaced flat electrodes have been shown to decrease MFC performance, despite a reduction in ohmic resistance, due to oxygen crossover from the anode to cathode [12]. However, it is possible to avoid decreases in power production with closely spaced electrodes by using a graphite fiber brush anode rather than a flat anode [13,14]. The relatively thick brush structure likely precludes oxygen diffusion into the brush that would affect electricity generation by exoelectrogenic microorganisms. Very close spacing of the

* Corresponding author. Tel.: +1 814 863 7908.
E-mail address: blogan@psu.edu (B.E. Logan).

0378-7753/$ – see front matter © 2013 Elsevier B.V. All rights reserved.
http://dx.doi.org/10.1016/j.jpowsour.2013.10.081

electrodes can be obtained by placing a separator between the electrodes to avoid electrode contact and short-circuiting. This separator electrode assembly (SEA) configuration also enables both more compact packing of electrodes and reduces oxygen crossover into the liquid [13]. Adding a separator, however, can add ohmic resistance, which can decrease power generation as well as create pH gradients that decrease performance [15]. The importance of ohmic resistance to performance becomes more important when solutions have a low conductivity, like many wastewaters.

Comparisons of SEA designs with electrode configurations with closely-spaced, but separatorless designs (spaced electrode, SPA), have so far focused primarily on conditions which are much different than those that exist when treating domestic wastewater with an MFC. These comparisons have typically made with a single and readily biodegradable compound as the fuel (e.g. acetate), well buffered solutions that have high solution conductivities (>7 mS cm^{-1}) compared to wastewater (~1 mS cm^{-1}), high organic loadings, and reactors with relatively large electrode spacing (several centimeters) [16]. The low conductivity of a wastewater can increase internal resistance, but the relative contribution of this to total resistance depends on the magnitude of other components of internal resistance. A high organic loading can reduce the impact of oxygen crossover on anode performance, as high concentrations of readily degradable substrate enables bacteria on the cathode to rapidly remove oxygen diffusing through the cathode. As a result of all these differences, it is not clear whether SPA or SEA designs would be more useful for domestic wastewater treatment.

In order to better understand the impact of these two different electrode configurations on domestic wastewater treatment, we constructed and tested multi-anode MFCs. The SEA reactors had two layers of separators placed between the electrodes, while the SPA reactors had the edge of the brush anode a distance of only 0.8 cm from the cathode. MFC performance was evaluated in terms of maximum power output, coulombic efficiency, and COD removal. Dissolved oxygen concentrations were measured in the solutions in order to better understand the potential effect of oxygen crossover on performance. Computer simulations were also performed to examine the effects of the two electrode configuration on substrate and oxygen transport relative to overall performance.

2. Material and methods

2.1. Construction and operation of MFCs

Single-chamber, air-cathode MFCs (130 mL) were constructed as previously described [6]. Each reactor contained three graphite fiber brush anodes (Mill-Rose, Mentor, OH) and a single air-cathode (30 wt% wet-proofed carbon cloth, type B-1B, E-TEK) with a platinum catalyst (0.5 mg cm^{-2}) on the water side, and four diffusion layers on the air side [17]. The anodes were heat treated at 450 °C for 30 min and were connected together externally with a single copper wire. The electrode distances between the anode core and the cathode were 0.5 cm for the SEA configuration and 2.0 cm for the SPA configuration. The SEA electrodes were both pressed against the separators, while the edge of the brush anode was 0.8 cm from the edge of the cathode in the SPA configuration (Fig. 1). Two layers of textile separator (Amplitude Prozorb, Contec Inc.) made from 46% cellulose and 54% polyester (thickness = 0.3 mm; weight = 55 g m^{-2}) were used for the SEA reactor to prevent short-circuiting and to minimize oxygen crossover. The anode brush for SEA MFC was trimmed half to prevent possible contact between the anode and cathode through the separator.

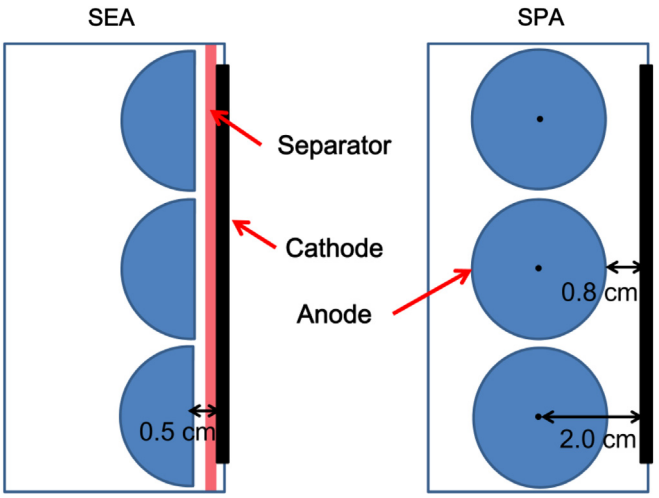

Fig. 1. Schematic of the MFCs with SEA and SPA configuration (not drawn to scale).

The MFCs were inoculated and fed with domestic wastewater from the primary clarifier of the Pennsylvania State University Wastewater Treatment Plant, and operated in fed-batch mode (duplicate reactors) at 30 °C in a constant temperature room. Reactors were refilled when the cell voltage decreased to <10 mV.

2.2. Analyses and calculations

The voltage (E) across an external resistor was measured every 20 min using a data acquisition system (Model 2700, Keithley Instruments) connected to a computer. Current (I) and power ($P = IE$) were calculated as previously described [1] and normalized by the projected surface area of the cathode (35 cm^2). Polarization and power density curves were obtained by varying the external resistance used in the circuit (3 batch cycles per resistor, multiple cycle method). Impedance measurements were taken from 1 MHz to 10 mHz by applying a sine wave (10 mV) on top of the bias potentials using a potentiostat (BioLogic, VMP3) under open circuit conditions. Total internal resistance (IR) was determined from the linear portion of the polarization data [1]. Ohmic resistance was determined from the first point of intersection of the x-axis in a Nyquist plot using electrochemical impedance spectroscopy (EIS) data [18]. Sum of the charge transfer and diffusion resistance was calculated as the difference between total IR and the solution resistance.

Coulombic efficiency (CE) was calculated using the ratio of the total coulombs produced during the experiment to the theoretical amount of coulombs available from the substrate as previously described [1]. COD was measured using a low range (0–150 mg L^{-1}) HACH COD system (Hach Co., Loveland, CO) [12]. Dissolved oxygen concentrations were measured using a non-consumptive oxygen probe (NeoFox, Ocean Optics Inc., Dunedin, FL).

2.3. Transport and electric field modeling

Simulations were conducted on both the SEA and SPA configurations using COMSOL Multiphysics (Version 4.2 (Palo Alto, CA)). A 2-D time dependent Poisson–Nernst–Planck model was evaluated under static conditions. Using this model, the substrate flux into each brush was examined over time. Anodes ($U_{a,0}$) and cathode potentials ($U_{c,0}$) were assumed (Table 1), and an induced electric field within the reactor was calculated (Eq. (1)):

Table 1
Parameters used during the constant anode potential simulations.

Variable	Symbol	Value	Units	Ref.
Dynamic viscosity	μ	1×10^{-3}	Pa s	[23]
Density	R	1000	kg m^{-3}	[23]
Anode potential	$U_{a,0}$	−0.2	V	Assumed
Cathode potential	$U_{c,0}$	0.1	V	Assumed
Substrate diffusion coefficient	D_s	1×10^{-9}	m^2 s^{-1}	[24]
Substrate mobility	$\mu_{m,s}$	1×10^{-13}	s mol kg^{-1}	OLI Analyzer 3.2
Charge number	z_s	−1		
Initial substrate concentration	$C_{sub,0}$	3.6	mol m^{-3}	Experiments
Oxygen concentration at cathode boundary	C_{O_2}	0.018	mol m^{-3}	Assumed
Oxygen diffusion coefficient through cathode	$D_{O_2,c}$	2×10^{-8}	m^2 s^{-1}	[19]
Oxygen diffusion coefficient through cathode with separator	$D_{O_2,s}$	4×10^{-10}	m^2 s^{-1}	[19]
Oxygen diffusion coefficient in anolyte	$D_{O_2,ano}$	4×10^{-9}	m^2 s^{-1}	[23]
Inlet velocity	v_o	5.4×10^{-6}	m s^{-1}	Experiments
Anolyte conductivity	σ	0.1	S m^{-1}	Experiments
Current	I	1	mA	Experiments
Faraday's constant	F	96,485	C mol^{-1}	
Simulation time step	dt	1000	s	
Ratio of the moles of acetate to moles of oxygen needed for aerobic oxidation	Y_{sub/O_2}	0.5	mol-Ac mol-O_2^{-1}	[25]

$$\boldsymbol{E} = -\nabla U \tag{1}$$

where $\boldsymbol{E}$ is electric field, and U is the voltage. The electric field was then used to solve the ionic current by:

$$\boldsymbol{J} = \left(\sigma + \varepsilon_0 \varepsilon_r \frac{\partial}{\partial t}\right)\boldsymbol{E} \tag{2}$$

where $\boldsymbol{J}$ is the current density, ε_o and ε_r are the relative permittivity of a vacuum and of the material used. The potential distribution was then used to solve for the ion concentration distribution within the anodes and anolyte using the Nernst–Planck equation:

$$\frac{\partial c_{sub}}{\partial t} + \nabla \cdot \left(-D_s \nabla c_s - z_s u_{m,s} F c_s \nabla U\right) + \mathbf{u} \cdot \nabla c_s = R_i \tag{3}$$

where c_s is the substrate concentration, D_s is the diffusivity of the substrate, z_s is the charge on the substrate, $u_{m,s}$ is the mobility of the substrate, F is the Faraday's constant, $\mathbf{u}$ is the velocity field and R is the reaction rate at the electrode due to current and the aerobic losses. The reaction rate due at the electrodes was determined through the use of a known current density which was established in the actual reactor. From this current, the reaction rate could be calculated as:

$$R_{s,cur} = \frac{I}{nF} \tag{4}$$

where I is the current, n is the number of electrons transferred. No-flux boundary conditions were applied to all boundaries except the inlet and outlet. Oxygen transfer into the anolyte was modeled using the diffusion–reaction equation:

$$\frac{\partial c_{O_2}}{\partial t} = D_{O_2,i}\left(\nabla^2 c_{O_2}\right) \tag{5}$$

where the diffusion coefficient ($D_{O_2,i}$) was estimated using mass transfer coefficients ($\mathbf{k}$, where $D = \mathbf{k}L$, and L is the diffusion length) previously obtained from cathodes, and the subscript i indicates diffusion through the cathode, cathode with separator, and anolyte [19]. The rate of substrate oxidation due to aerobic growth due to the presence of oxygen in the reactor was calculated as

$$R_{sub,O_2} = \left(Y_{sub/O_2}\frac{c_{O_2}}{dt}\right) \tag{6}$$

where dt was the time step taken during the transient simulation, and Y_{sub/O_2} was the stoichiometric ratio of the moles of acetate to the moles of oxygen needed for aerobic oxidation.

3. Results and discussion

3.1. Power production

There was no appreciable difference in start-up time between SEA and SPA configurations. SEA MFCs produced maximum voltage of 0.58 V (R_{ext} = 1000 Ω) after 2.9 days, and SPA MFCs produced 0.54 V after 3.4 days following inoculation (data not shown). Polarization tests based on the multiple-cycle method were conducted after 20 days to obtain power density curves, with no evidence of power overshoot. SEA MFCs produced a maximum power density of 328 ± 11 mW m^{-2}, which was slightly higher than that produced with SPA configuration of 282 ± 29 mW m^{-2} (Fig. 2). These values were higher than those previously obtained with the SEA reactor and domestic wastewater (120 mW m^{-2}) [20], likely due to variations in wastewater composition and the higher influent COD concentration here (303 ± 69 mg L^{-1}, compared to 275 ± 71 mg L^{-1} previously). The SPA configuration was not previously examined with wastewater.

3.2. COD removal, coulombic efficiency, and energy recovery

The electrode design did not influence the extent of COD removal, although the time needed for this COD removal varied. Total COD removal ranged from 62 ± 4% to 94 ± 1% with SEA MFCs, and compared to 81 ± 5% to 93 ± 3% with SPA MFCs (Fig. 3A). These values were similar to those obtained using the same domestic wastewater source with the SEA configuration [13,20]. There was a larger difference in CEs for the two designs. The CE with the SPA

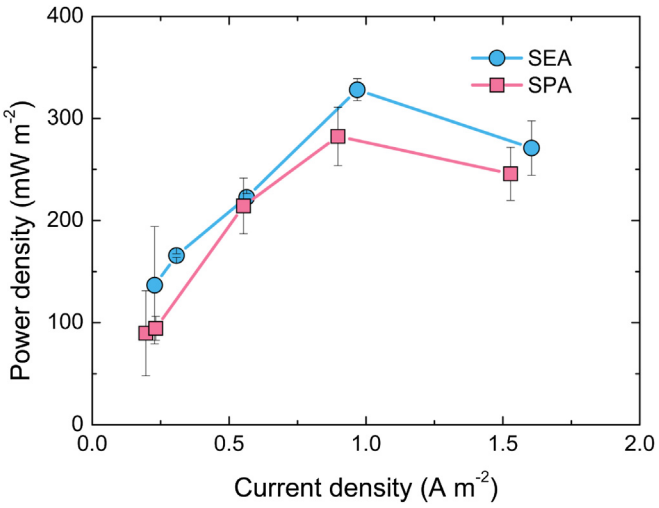

Fig. 2. Power density curves for SEA and SPA configuration MFCs fed with domestic wastewater.

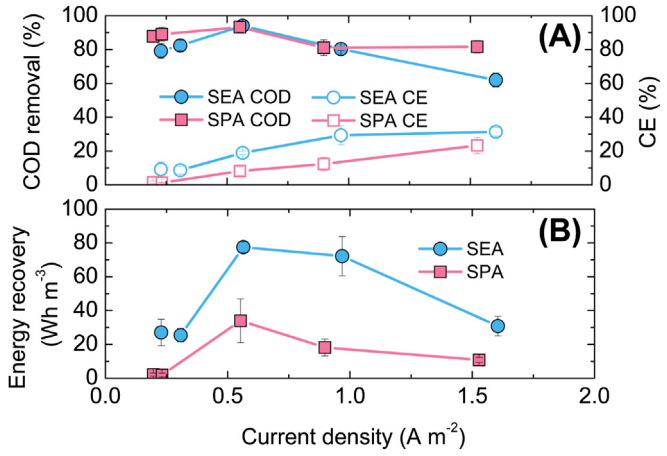

Fig. 3. (A) COD removal, CEs, and (B) normalized energy recoveries for SEA and SPA configuration MFCs fed with domestic wastewater.

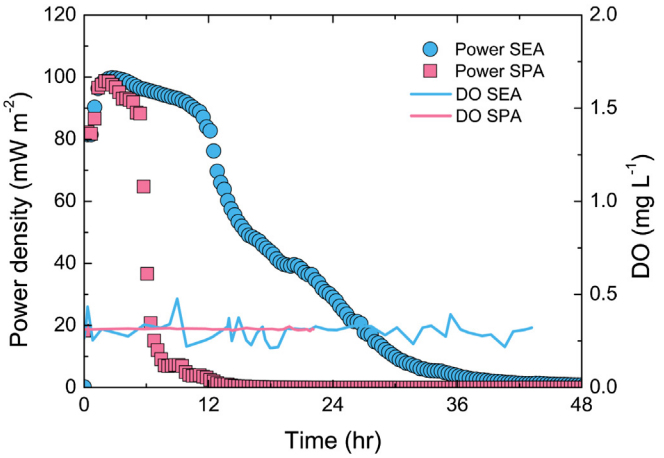

Fig. 4. Power output and DO concentration for SEA and SPA configuration MFCs fed with domestic wastewater (R_{ext} = 1000 Ω) over a complete fed-batch cycle.

configuration was only 1.5 ± 0.7% at 0.2 A m^{-2} (Fig. 3A), although it increased with current [15] to a maximum of 23.3 ± 4.8% at 1.5 A m^{-2}. In the SEA configuration, the CEs were higher and increased from 9.2 ± 4.4% at 0.2 A m^{-2} to 31.4 ± 2.6% at 1.6 A m^{-2}. The MFCs with the SEA configuration had an energy recovery up to 78 ± 3 Wh m^{-3}, compared to 34 ± 13 Wh m^{-3} with the SPA configuration (Fig. 3B). The lower CEs and energy recoveries with the SPA configuration, despite similarly high COD removals as the SEA, indicated that only a small portion of organic matter could be captured as current.

The main difference in the two configurations was that the SEA design required a much longer time for wastewater treatment (Fig. 4 and Fig. S1). During a batch cycle (R_{ext} = 1000 Ω), SPA MFCs produced power between 90 and 100 mW m^{-2} for a period of 6 h with total

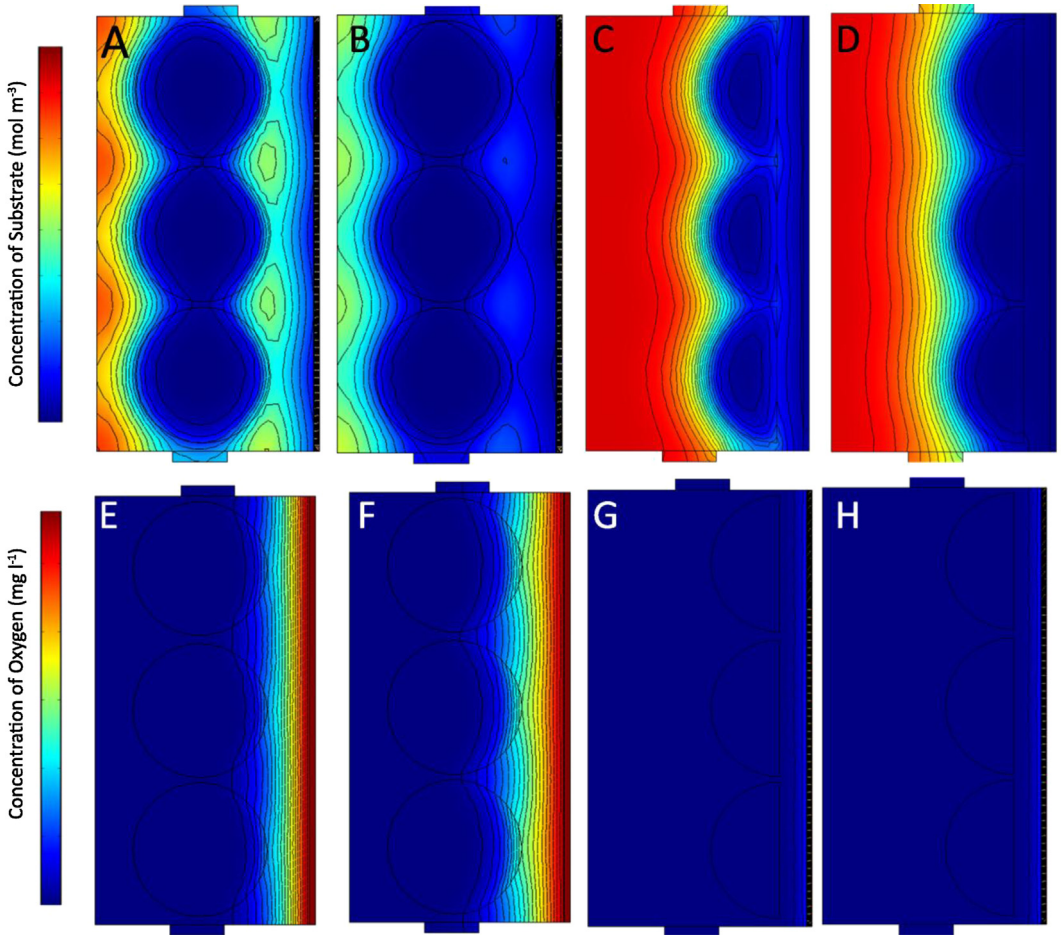

Fig. 5. Substrate distribution through SEA and SPA reactor in batch mode in SPA at (A) 6 h, and (B) 12 h, and in SEA at (C) 6 h, and (D) 12 h. Oxygen concentrations through SEA and SPA reactor are also displaced in SPA (E) 6 h, (F) 12 h, and SEA at (G) 6 h, and (H) 12 h.

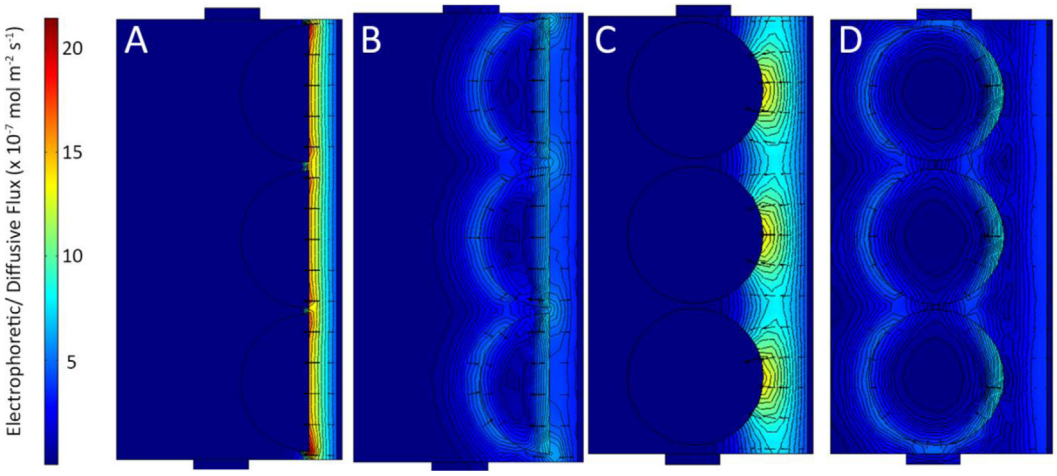

Fig. 6. The electrophoretic flux (A, C) in SEA and SPA reactors, and diffusive flux (B, D) in SEA and SPA reactors at ~2.5 h.

cycle time of 12 h, while the SEA required a much longer cycle time of 36 h (Fig. 4). This indicates that the higher CEs with SEA were due to the longer cycle time, and not from the improvement in electrode performance. The SEA configuration had a separator, which reduced the overall oxygen intrusion into the anode chamber. This led to less substrate consumption due to the aerobic oxidation with the SEA configuration, also contributing to the longer cycle time with the SEA. This difference in time needed for treatment and the low CEs indicated that non-exoelectrogenic bacteria played an important role in organic removal in both configurations.

From the perspective of wastewater treatment, the SPA configuration was superior to the SEA design as it produced the same level of wastewater treatment as the SEA configuration, but in less time.

3.3. Dissolved oxygen concentration and internal resistance

In order to better understand the reasons for difference in performance between two configurations, dissolved oxygen concentrations near the anode were measured during a fed-batch cycle (Fig. 4). The oxygen concentration in the anode solution was 0.30 ± 0.05 mg L^{-1} over 43 h for the SEA MFC, and essentially the same as that obtained for the SPA MFC (0.31 ± 0.01 mg L^{-1}) over 22 h. Although oxygen intrusion through the cathode to anode can inhibit current generation [9], it may be that these concentrations were too low to impact performance. However, in the SEA configuration, the oxygen concentration could be higher in the portion of the anode next to the separator as suggested by previous studies [21,22].

The total internal resistances determined from the slope of the polarization curve were the same at 64 Ω for both configurations, in agreement with power density results that both configurations produced a similar maximum power density (Fig. 4). With the SPA design, the ohmic resistance was 16 Ω. By using an SEA configuration, the ohmic resistance decreased to 9 Ω even though two separators were used between the electrodes. However, the use of the SEA configuration increased the sum of diffusion and charge transfer resistances to 55 Ω, which was larger than that obtained for the SPA configuration (48 Ω). In the SEA configuration, the substrate can diffuse to only one side of the brush anode as there is essentially no space between the anode and cathode, thus resulting in higher diffusion resistance compared to that for the SPA configuration. This could lower the substrate flux to the brush anode, and increase the cycle time for SEA MFCs relative to the SPA configuration (Fig. 4).

3.4. Simulation results for substrate diffusion into SPA and SEA brush anodes

Under batch conditions, diffusion (substrate gradients) and electromigration (voltage gradients that move negatively charged

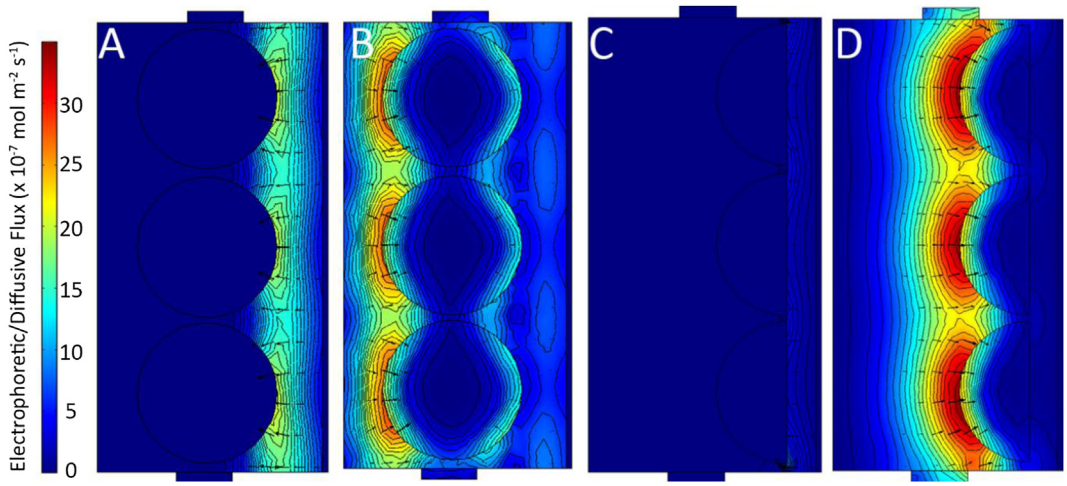

Fig. 7. The electrophoretic flux (A, C) SEA and SPA reactor, and diffusive flux (B, D) in SEA and SPA reactors at ~12 h.

substrate towards the anode) drive charged volatile fatty acids (VFAs) such as acetate, butyrate, and propionate from the bulk solution into the brush where they are oxidized by bacteria. Oxygen can diffuse through the cathode into the bulk solution where it is used by bacteria for the oxidation of organic matter, reducing coulombic efficiency. A clear advantage of the SEA configuration was the decrease in the oxygen mass transfer coefficient through the cathode by nearly two orders of magnitude. From the simulations, it is evident that the substrate located in between the electrodes would be depleted early during the batch cycle for both reactors (Fig. 5). After 6 h for the SPA reactor, simulations indicate that the bulk anolyte near the cathode contained ~1–2 mol m^{-3} of substrate, whereas the region furthest from the cathode had ~3 mol m^{-3}. After 12 h, nearly all of the substrate in between the anode and cathode would be depleted for both the SPA and SEA reactors (Fig. 5B and D). For the SPA configuration, which lacks a separator, this removal of substrate near the cathode was in part due to the higher concentration of oxygen that is present within this region of the reactor (Fig. 5E and F). With the SEA reactor, a much smaller amount of substrate would be removed as a result of oxygen intrusion into the anolyte (Fig. 5G and H).

Assuming that biofilms on each brush produced the same current and voltage, the generated electric field would remain even in the region in between the electrodes (Fig. S2). As the distance between the anode and cathode was decreased using the SEA arrangement, the area of the reactor exposed to the electric field would decrease, but the strength of the electric field would increase. The electric field strength has an effect on the electromigration of charged substrates such as VFAs, and this is visible through the electrophoretic flux generated in each reactor (Fig. 6A and C). During the initial hours of the batch, the electrophoretic flux within the electric field is greater than the diffusive flux (Fig. 6B and D). However, outside of the electric field, diffusion is the dominate means by which substrate is transported to the biofilm. Thus, the depletion of the substrate in between the electrodes for the SEA reactor maybe attributed to the higher electrophoretic flux. Later within the fed batch cycle, after substrate near the cathode was depleted either due to oxygen intrusion (SPA) or greater electrophoretic fluxes (SEA), diffusion would become the dominate transport process throughout the reactor (Fig. 7).

4. Conclusions

Reducing the distance between the electrodes using the SEA design improved performance in terms of power production (328 mW m^{-2}), CE (9.2–31.4%), and energy recovery (25–78 Wh m^{-3}) compared to the SPA design (282 mW m^{-2}, 1.5–23.3%, 2–34 Wh m^{-3}) without appreciable differences in COD removals. However, the improved performance greatly increased treatment time (36 h for SEA, 12 h for SPA) likely due to the hindered oxygen intrusion into the anode, and reduced substrate diffusion into the SEA brush. As the cost of an MFC reactor can be quite important, this suggests that the SPA design is more practical for effective wastewater treatment despite a low CE than the SEA. However, the SEA configuration may be desirable if the objective is high conversion rates of fuel to current.

Acknowledgments

The research reported here was supported by the King Abdullah University of Science and Technology (KAUST) (Award KUS-I1-003-13).

Appendix A. Supplementary data

Supplementary data related to this article can be found at http://dx.doi.org/10.1016/j.jpowsour.2013.10.081.

References

[1] B.E. Logan, B. Hamelers, R.A. Rozendal, U. Schrorder, J. Keller, S. Freguia, P. Aelterman, W. Verstraete, K. Rabaey, Environ. Sci. Technol. 40 (2006) 5181–5192.
[2] D. Pant, G. Van Bogaert, L. Diels, K. Vanbroekhoven, Bioresour. Technol. 101 (2010) 1533–1543.
[3] K. Rabaey, W. Verstraete, Trends Biotechnol. 23 (2005) 291–298.
[4] D. Jiang, X. Li, D. Raymond, J. Mooradain, B. Li, Int. J. Hydrogen Energy 35 (2010) 8683–8689.
[5] A. Dekker, A. Ter Heijne, M. Saakes, H.V.M. Hamelers, C.J.N. Buisman, Environ. Sci. Technol. 43 (2009) 9038–9042.
[6] Y. Ahn, B.E. Logan, Appl. Microbiol. Biotechnol. 93 (2012) 2241–2248.
[7] J.M. Sonawane, A. Gupta, P.C. Ghosh, Int. J. Hydrogen Energy 38 (2013) 5106–5114.
[8] G.G. Kumar, V.G.S. Sarathi, K.S. Nahm, Biosens. Bioelectron. 43 (2013) 461–475.
[9] X.Y. Zhang, S.A. Cheng, X. Wang, X. Huang, B.E. Logan, Environ. Sci. Technol. 43 (2009) 8456–8461.
[10] M.M. Ghangrekar, V.B. Shinde, Bioresour. Technol. 98 (2007) 2879–2885.
[11] J.C. Biffinger, R. Ray, B. Little, B.R. Ringeisen, Environ. Sci. Technol. 41 (2007) 1444–1449.
[12] S. Cheng, H. Liu, B.E. Logan, Environ. Sci. Technol. 40 (2006) 2426–2432.
[13] S. Hays, F. Zhang, B.E. Logan, J. Power Sources 196 (2011) 8293–8300.
[14] A.J. Hutchinson, J.C. Tokash, B.E. Logan, J. Power Sources 196 (2011) 9213–9219.
[15] J.R. Kim, S. Cheng, S.E. Oh, B.E. Logan, Environ. Sci. Technol. 41 (2007) 1004–1009.
[16] Y. Fan, H. Hu, H. Liu, J. Power Sources 171 (2007) 348–354.
[17] S. Cheng, H. Liu, B.E. Logan, Electrochem. Commun. 8 (2006) 489–494.
[18] Z. He, F. Mansfeld, Energy Environ. Sci. 2 (2009) 215–219.
[19] H. Liu, B.E. Logan, Environ. Sci. Technol. 38 (2004) 4040–4046.
[20] Y. Ahn, B.E. Logan, Appl. Microbiol. Biotechnol. 97 (2013) 409–416.
[21] Z. Wang, H. Deng, L. Chen, Y. Xiao, F. Zhao, Bioresour. Technol. 132 (2013) 387–390.
[22] Y. Yuan, S. Zhou, J. Tang, Environ. Sci. Technol. 47 (2013) 4911–4917.
[23] B.E. Logan, Environmental Transport Processes, John Wiley & Sons, Inc., 2012.
[24] C. Picioreanu, I.M. Head, K.P. Katuri, M.C.M. van Loosdrecht, K. Scott, Water Res. 41 (2007) 2921–2940.
[25] B.E. Rittmann, P.L. McCarty, Environmental Biotechnology: Principles and Applications, McGraw-Hill, 2001.